Higher-order triplet interaction in energy-level modeling of excited-state absorption for an expanded porphyrin cadmium complex

Michael M. McKerns,* Wenfang Sun,† and Chris M. Lawson

Laser and Photonics Research Center, Department of Physics, University of Alabama at Birmingham, Birmingham, Alabama 35294

Gary M. Gray

Department of Chemistry, University of Alabama at Birmingham, Birmingham, Alabama 35294

Received February 20, 2004; revised manuscript received August 11, 2004; accepted October 25, 2004

Recent measurements of transmission versus fluence for a methanol-solvated asymmetric pentaazadentate porphyrin-like (APPC) cadmium complex, [(C_6H_4–APPC)Cd]Cl, showed the limitations of current energy-level models in predicting the transmission behavior of organic reverse saturable absorbers at fluences greater than 1 J/cm^2. A new model has been developed that incorporates higher-order triplet processes and accurately fits both nanosecond and picosecond transmission-versus-fluence data. This model has provided the first known determination of a higher triplet excited-state absorption cross section and lifetime for an APPC complex and also described a previously unreported feature in the transmission-versus-fluence data. The intersystem crossing rate and the previously neglected higher triplet excited-state absorption cross section are shown to govern the excited-state population dynamics of methanol-solvated [(C_6H_4–APPC)Cd]Cl most strongly at more-practical device energies.

OCIS codes: 190.0190, 190.4400, 160.4330, 160.4890, 160.6990.

1. INTRODUCTION

Nonlinear optical (NLO) materials with large and fast NLO responses are good candidates for the optical switches, optical rectification, and optical power-limiting applications of the near future.[1–4] Further, NLO materials with fast intersystem crossing (ISC) and long triplet lifetimes are suitable for current biomedical applications such as photodynamic therapy in the battle against cancer.[5,6] Excited-state absorption (ESA) and electronic polarization are known mechanisms for producing large and fast NLO responses in molecules[7–9]; however, it is not currently possible *a priori* to design molecules that have a strong ESA or a large electronic polarization response. Materials that exhibit reverse saturable absorption (RSA) are of particular interest because they commonly possess complex excited-state behavior and have direct applications to optical switching devices.[10] Reverse saturable absorbing chromophores typically exhibit a large ratio of effective excited-state absorption cross-section–ground-state absorption cross section; thus there is the potential for large nonlinear attenuation while low linear absorption is maintained.[11] In addition, because optical energy is generally absorbed and converted to heat, reverse saturable absorbing materials should be well suited for use in fast optical systems and sensor protection. The goal of this study is to provide a more-accurate method of characterizing ESA response in reverse saturable absorbing materials at more-practical device energies.

Asymmetric pentaazadentate porphyrin-like (APPC) complexes, such as [(C_6H_4–APPC)Cd]Cl (Fig. 1), are an important class of reverse saturable absorbing material. Much of the rationale for exploring the ground- and excited-state optical properties of APPC complexes began with the recognition that pentaazadentate porphyrin solutions absorb strongly in the spectral region near 755 nm.[5,12] This spectral region is of particular interest for use in photodynamic therapy because bodily tissues and blood are maximally transparent in that region.[6,12] Optical power limiting (OPL), *Z*-scan, and time-resolved degenerate four-wave mixing studies of APPC complexes have demonstrated that the excited-state population dynamics dominate the NLO responses of these complexes.[9,13–18] These measurements, however, provide information only about the ground and effective first excited states of the complexes.

One can obtain a more comprehensive characterization of excited-state absorbing materials by fitting the transmission-versus-fluence data to a set of rate equations that describe the time-dependent populations in the various electronic levels. In 1967 a detailed study[19] of the transmission characteristics of saturable absorbers showed the inadequacy of a two-level model to describe the RSA that occurs in solutions of sudanschwartz-B and sulfonated indanthrone. This study concluded that materials that show RSA tend to retain population in one of the excited states of the molecule and, thus, require more energy levels for describing the transmission behavior. In 1994 Si *et al.*[9,20] fitted the OPL performance of cadmium texaphyrin {a pentaazadentate porphyrin complex that is very closely related to [(C_6H_4–APPC)Cd]Cl} in ac-

0740-3224/2005/040852-10$15.00

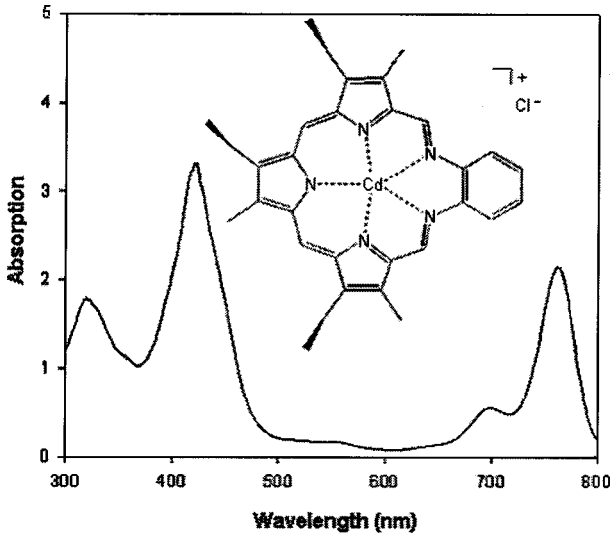

Fig. 1. Chemical structure of [(C_6H_4–APPC)Cd]Cl and linear absorption spectrum of a 4.33×10^{-4} mol/L methanol solution of [(C_6H_4–APPC)Cd]Cl in a 2-mm cell.

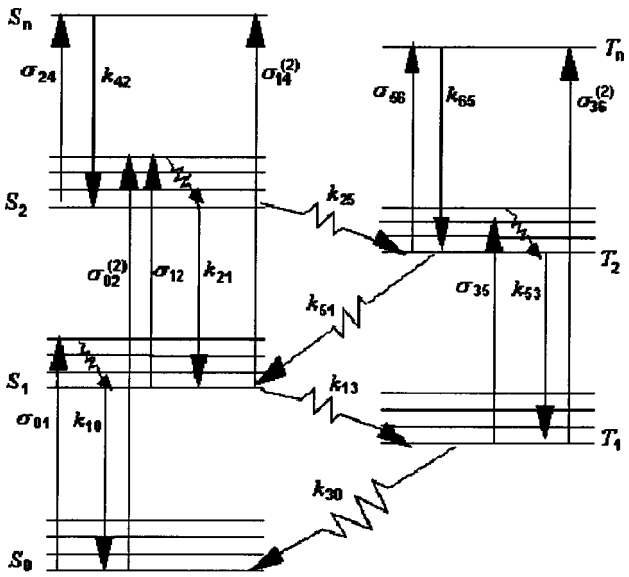

Fig. 2. Seven-state energy-level model of nonlinear absorption. Each of the electronic energy levels has a manifold of vibrational and rotational sublevels associated with it; however, for metal-organic reverse saturable absorbing molecules these sublevels have negligible effect. Single- and two-photon absorption cross sections [σ_{ij} and $\sigma_{ik}^{(2)}$] or decay rates (k_{ji}) shown are representative of the labeled energy-level transition.

etonitrile to a six-level model under the approximation that both the uppermost excited singlet and the second (and higher) excited triplet states of cadmium texaphyrin have negligible lifetimes. Si *et al.* found that, whereas picosecond pulses utilized the first and second singlet excited states, for nanosecond pulses only the first excited triplet state was shown to have an effect on the transmission curve.[9] These results, however, were limited by the inherent approximations made in their model.

Another significant limitation of the study of Si *et al.* is that only relatively low fluences were used in fitting the transmission-versus-fluence data. We recently measured the transmission-versus-fluence data for [(C_6H_4–APPC)Cd]Cl at significantly higher fluences[13,14] and found that the model developed by Si *et al.* does not adequately describe the OPL behavior of [(C_6H_4–APPC)Cd]Cl at high fluences. The seven-state energy-level model (Fig. 2) presented in this paper successfully describes the excited-state absorption of [(C_6H_4–APPC)Cd]Cl at both high and low fluences and, further, does not assume negligible upper excited-state lifetimes or neglect the potential for two-photon transitions. In addition, a critical new step is taken in this manuscript, in which the transition rates are recognized as separable not only by spin character but by fluence.

2. EXPERIMENT

[(C_6H_4–APPC)Cd]Cl (Fig. 1) was synthesized by a procedure described in the literature.[21–24] The complex was characterized by UV–visible, IR, ^{1}H-NMR, and fast atom-bombardment mass spectroscopy[22] methods; elemental analysis was also conducted to verify the purity of the sample.[24] All measurements for this manuscript were made of a 4.33×10^{-4} mol/L methanol solution of [(C_6H_4–APPC)Cd]Cl. The linear absorption[13,25] and transient difference spectra,[26] the lifetimes of first excited states,[26,27] the quantum yield of the first triplet excited state,[26] and the ISC rate[27] had all been previously determined. The OPL curve for the [(C_6H_4–APPC)Cd]Cl solution was obtained by use of a standard nonlinear transmission technique[10,13] in which a 5-ns laser pulse or, alternatively, a 40-ps laser pulse was used as a light source ($\lambda = 532$ nm) for the OPL measurements. For the nanosecond pulses the laser beam was focused at the center of a 2-mm path-length quartz cell by a 25-cm

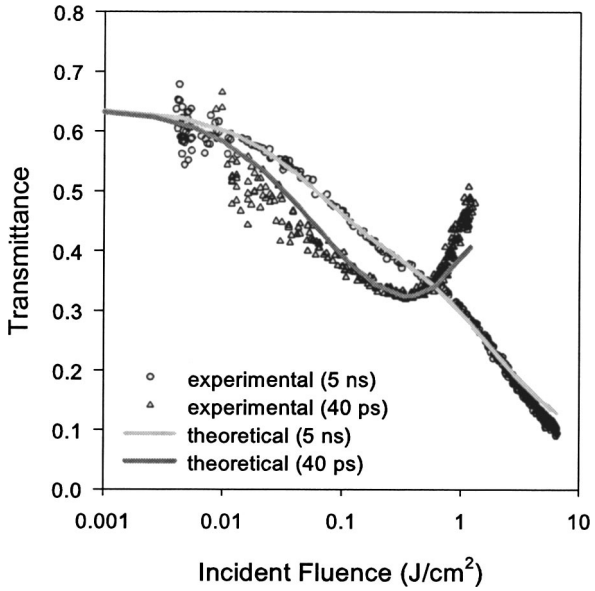

Fig. 3. Transmission versus incident fluence at 532 nm for a 4.33×10^{-4} mol/L methanol solution of [(C_6H_4–APPC)Cd]Cl for two pulse durations. The extension of the measured fluence to greater than 1 J/cm^2 compelled the addition of higher-order triplet transitions to permit more-accurate modeling of methanol-solvated [(C_6H_4–APPC)Cd]Cl at these more-practical device energies.

plano–convex lens ($f/38$), resulting in a $1/e^2$ spot radius of ~195 μm; for the picosecond laser pulses a 30-cm plano–convex lens ($f/146$) was used to focus the beam to a waist radius of ~65 μm. To ensure that no hysteresis or cell damage occurred we cycled through the full range of energies multiple times; we also discounted solution burning and decomposition by measuring the linear absorption spectrum before and after the OPL measurements. *Z*-scan measurements (40 ps and 5 ns at 532 nm) showed the [(C_6H_4–APPC)Cd]Cl solution to have negligible thermal lensing[16,17] and provided approximations of the total excited-state absorption cross section, σ_e.

Transmission curves (for both 40-ps and 5-ns pulses) for solutions of [(C_6H_4–APPC)Cd]Cl initially exhibit RSA for input fluences greater than ~0.01 J/cm^2, and the transmission decreases steadily until ~0.1 J/cm^2 (Fig. 3). For 40-ps pulses, the slope of the transmission curve becomes less negative until RSA ceases at ~0.3 J/cm^2, after which transmission begins to increase with incident fluence. For 5-ns pulses, RSA occurs even at the highest energies; however, the corresponding transmission curve experiences a slight dip centered at approximately 0.3 J/cm^2, marking a transition between two different slopes.

3. THEORETICAL MODEL

A. Description of the Energy-Level Model

A seven-state energy-level model (Fig. 2) provides an excellent description of the nonlinear transmission behavior of metalloporphyrin-like molecules on nanosecond and picosecond time scales over a wide range of pulse energies.[28] Half of the energy-level system comprises ground state S_0, first singlet excited state S_1, second singlet excited state S_2, and an upper singlet excited state S_n; first triplet excited state T_1, second triplet excited state T_2, and upper triplet excited state T_n complete the other half of the model. Each of these electronic energy levels has a manifold of vibrational and rotational sublevels associated with it; however, for metal-organic reverse saturable absorbing molecules these vibrational and rotational sublevels can be ignored owing to the neglect of coherence effects (dephasing) and the assumption of ultrafast relaxation of vibronic sublevels.[10,29,30] To investigate quantitatively the resonant and nonresonant interaction between the nonlinear medium and the incident laser light, we track the time variation of the population density for the seven-state energy-level model through use of a rate equation:

$$\frac{d\mathbf{N}}{dt} = \hat{R}\mathbf{N}, \tag{1}$$

$$\mathbf{N} = |N_0\ N_1\ N_2\ N_3\ N_4\ N_5\ N_6|. \tag{2}$$

Population vector $\mathbf{N}$ is composed of the population densities of all seven levels; N_0, N_1, N_2, N_3, N_4, N_5, and N_6 correspond to the population densities in S_0, S_1, S_2, T_1, S_n, T_2, and T_n, respectively. Rate operator $\hat{R}$ can be expressed by

$$\hat{R} = \begin{bmatrix} -\sigma_{01}\Phi & k_{10} & 0 & k_{30} & 0 & 0 & 0 \\ \sigma_{01}\Phi & -k_{10}-k_{13}-\sigma_{12}\Phi & k_{21} & 0 & 0 & 0 & 0 \\ 0 & \sigma_{12}\Phi & -k_{21}-\sigma_{24}\Phi & 0 & 0 & 0 & 0 \\ 0 & k_{13} & 0 & -k_{30}-\sigma_{35}\Phi & 0 & k_{53} & 0 \\ 0 & 0 & \sigma_{24}\Phi & 0 & 0 & 0 & 0 \\ 0 & 0 & 0 & \sigma_{35}\Phi & 0 & -k_{53}-\sigma_{56}\Phi & 0 \\ 0 & 0 & 0 & 0 & 0 & \sigma_{56}\Phi & 0 \end{bmatrix} + R', \tag{3}$$

$$R' = \begin{bmatrix} -\sigma_{02}^{(2)}\Phi I & 0 & 0 & 0 & 0 & 0 & 0 \\ 0 & -\sigma_{14}^{(2)}\Phi I & 0 & 0 & 0 & k_{51} & 0 \\ \sigma_{02}^{(2)}\Phi I & 0 & -k_{25} & 0 & k_{42} & 0 & 0 \\ 0 & 0 & 0 & -\sigma_{36}^{(2)}\Phi I & 0 & 0 & 0 \\ 0 & \sigma_{14}^{(2)}\Phi I & 0 & 0 & -k_{42} & 0 & 0 \\ 0 & 0 & k_{25} & 0 & 0 & -k_{51} & k_{65} \\ 0 & 0 & 0 & \sigma_{36}^{(2)}\Phi I & 0 & 0 & -k_{65} \end{bmatrix} \tag{4}$$

in terms of single- and two-photon absorption cross sections [σ_{ij} and $\sigma_{ik}^{(2)}$], decay rates (k_{ji}), and photon flux ($\Phi = I/h\nu$). Total population density N is conserved for the seven-state energy-level system and can be represented by

$$N = \sum_{i=0}^{6} N_i(t), \tag{5}$$

$$N_i(t = -\infty, z) = N\delta_{0i}, \tag{6}$$

where Dirac delta function δ_{0i} allows for the expression of the initial population densities of each state. A light-propagation equation,

$$\frac{dI}{dz'} = -\alpha I - \beta I^2, \tag{7}$$

Table 1. Absorption Cross Sections for [(C$_6$H$_4$–APPC)Cd]Cl in Methanol

Cross Section	Value (cm^2)
σ_{01}	8.8×10^{-18}[a]
σ_{35}	2.0×10^{-17}
σ_{56}	2.8×10^{-16}
σ_{12}	3.1×10^{-17}
σ_{24}	$\leq 1.0 \times 10^{-19}$

[a] Calculated from linear transmittance; $\sigma_{01} \approx -\ln(T_{\text{lin}})/\text{NL}$.

Table 2. Decay Rates for [(C$_6$H$_4$–APPC)Cd]Cl in Methanol

Decay Rate	Value (s^{-1})
k_{10}	2.6×10^{8}[a]
k_{13}	2.6×10^{9}[a]
k_{30}	5.6×10^{4}[b]
k_{21}	5.0×10^{11}
k_{53}	1.2×10^{11}

[a] Measured in Ref. 27.
[b] Measured in Ref. 26.

$$\alpha = \sigma_{01}N_0 + \sigma_{12}N_1 + \sigma_{24}N_2 + \sigma_{35}N_3 + \sigma_{56}N_5, \quad (8)$$

$$\beta = [\sigma_{02}^{(2)}N_0 + \sigma_{14}^{(2)}N_1 + \sigma_{36}^{(2)}N_3]/h\nu, \quad (9)$$

is used to describe the variation of light intensity through the sample, where the incident laser pulse $I(t, z = 0)$ is assumed to be of Gaussian spatial and temporal profile and the slowly varying envelope approximation has been invoked.

B. Implementation

A computer program was written for a numerical solution of the full, coupled rate-equation expression for the system. By assuming that the spatial profile has a limited effect on the absorption dynamics, we condensed the Gaussian spatial term into the value at FWHM. We made further simplifications by initially assuming negligible two-photon transitions and upper ISC rates and by neglecting the populations of upper excited states S_n and T_n because we assumed rapid relaxation. Electronic energy levels not accessible through laser excitation at 532 nm (with the exception of T_1) were also neglected.

An iterative procedure was used to fit the rate parameters to the transmission curves (Fig. 3). To improve the accuracy of fitting to noisy data, we smoothed the transmission data to create a representative curve; the curve

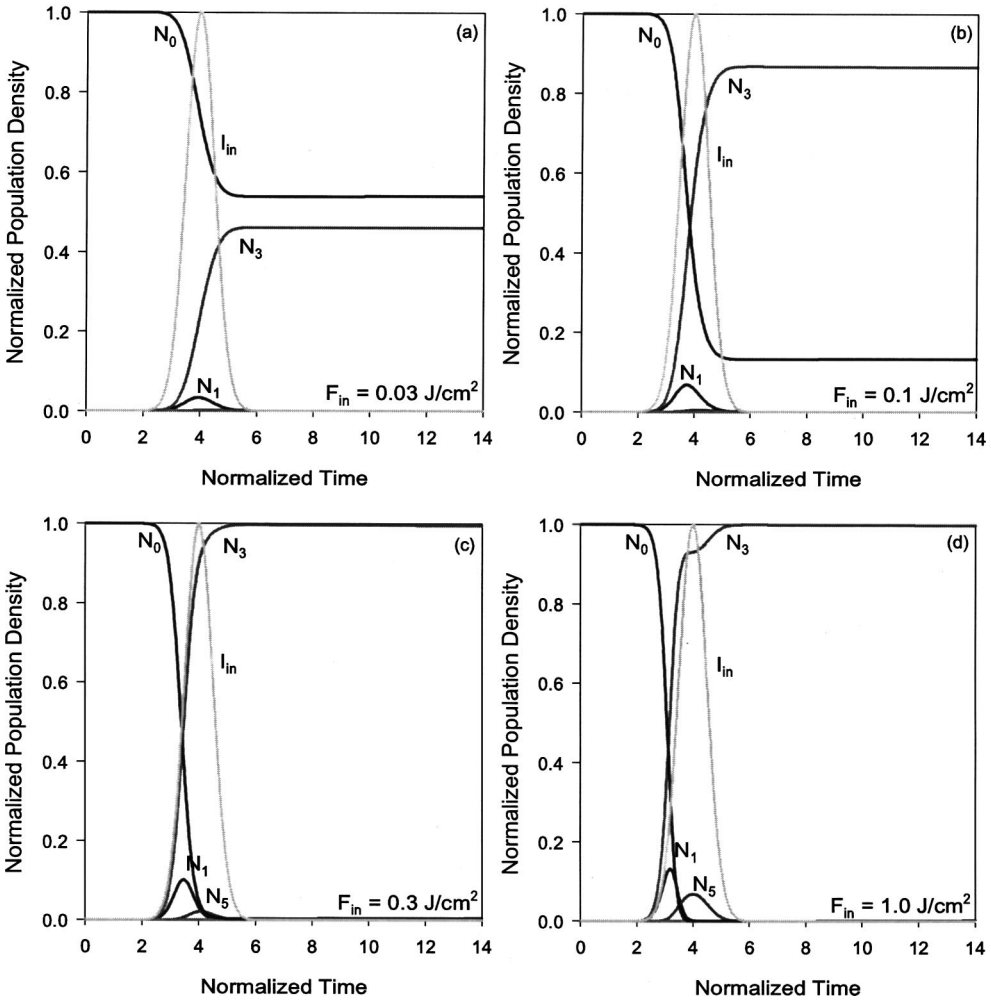

Fig. 4. Dynamics of population density at 5 ns and 532 nm for a 4.33×10^{-4} mol/L methanol solution of [(C$_6$H$_4$–APPC)Cd]Cl. Normalized incident pulse intensity (I_{in}) and normalized population density are shown for each electronic energy level and for four input fluences F_{in}.

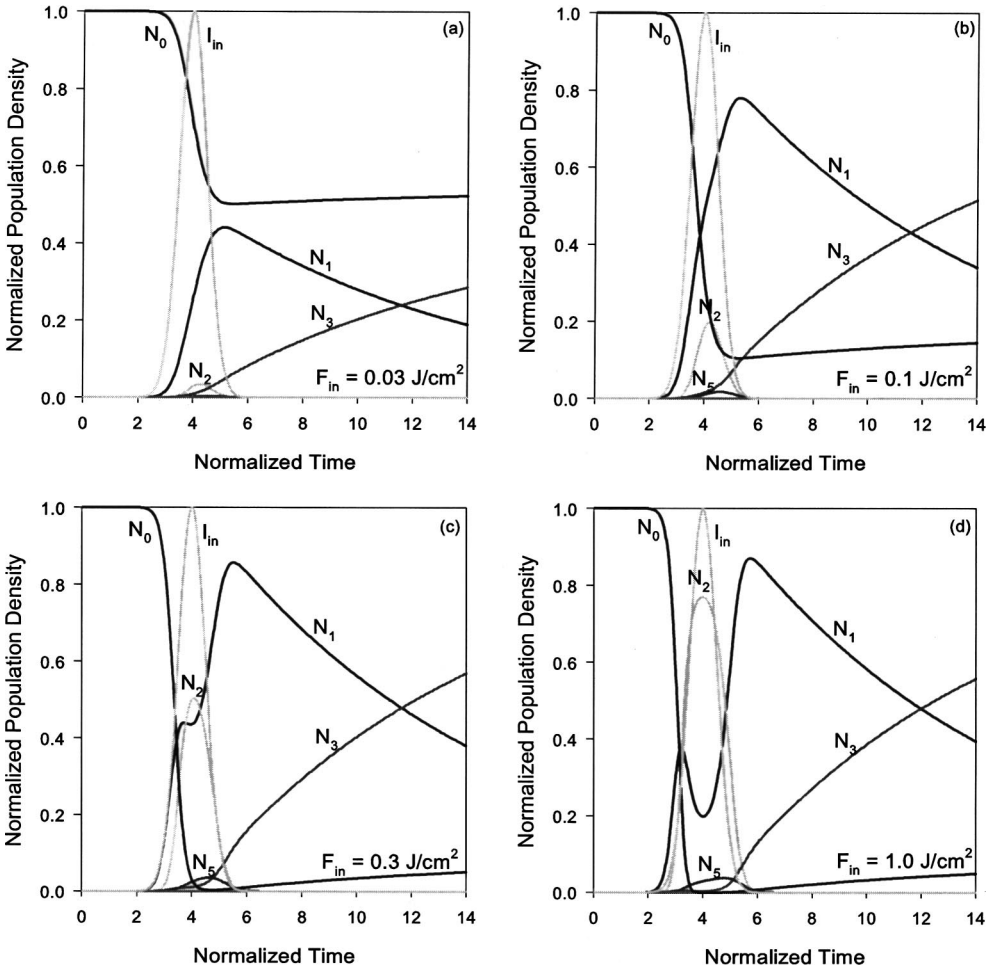

Fig. 5. Dynamics of population density at 40 ps and 532 nm for a 4.33×10^{-4} mol/L methanol solution of [(C_6H_4–APPC)Cd]Cl. Normalized incident pulse intensity (I_{in}) and normalized population density are shown for each electronic energy level and for four input fluences F_{in}.

was then normalized by the linear transmittance, T_{lin}. The parameters k_{13}, k_{30}, k_{10}, and σ_{01} were then taken from fluorescence,[26,27] transient absorption,[26] and linear transmission data; we approximated first triplet excited-state absorption cross section σ_{35} by fitting the nanosecond data in the 0.001–0.3 J/cm^2 range under the assumption that $\sigma_{12} = \sigma_e$ (as measured by a Z scan at 40 ps).[16,17] Then, using the newly calculated σ_{35}, we fitted the RSA portion of the picosecond data to obtain a more-precise value for σ_{12}. Next, σ_{56} and k_{53} were evaluated and the fit of σ_{35} was refined over the duration of the nanosecond curve. Utilizing these newly calculated values, we extracted σ_{24} and k_{21} and recalculated σ_{12} to best fit the whole length of picosecond data. Where necessary, another iterative cycle was then performed to produce the final values of all absorption cross sections (Table 1) and decay rates (Table 2).

4. RESULTS AND DISCUSSION

A. Testing the Parameter Basis

We then tested the initially neglected parameters, one at a time, by adding them from R' to the simulation and repeating the above process; thus, both the presence of two-photon transitions, intersystem crossings between higher singlet and triplet excited states, and the possibility of nonnegligible upper excited-state lifetimes were also explored in this model. Models currently reported in the literature attempt only to track the behavior of k_{13} and k_{30} and do not typically include these rates as fit parameters. Adding k_{25} as a fit parameter was a further attempt to expand the fitting ability of the present model; however, k_{25} was found to have a negligible effect for the complex studied. The addition of k_{65} and k_{42} was similarly found to produce a negligible effect for [(C_6H_4–APPC)Cd]Cl. The k_{51} transition was also considered but was omitted because of the likelihood of a large energy gap between T_2 and S_1.

All energy levels considered (with the exception of T_1) were accessible by means of one- or two-photon excitation by a laser at 532 nm; thus, for the model presented in this manuscript, the energy-level separation is approximately the same within a same-spin system. This model, however, does not account for the possibility of intermediate electronic energy levels that lie between the seven levels shown. The linear absorption and transient difference spectra for [(C_6H_4–APPC)Cd]Cl show that most likely there exist electronic energy levels in addition to those used in this model.[13,25,26] However, if all spin–flip transitions (intersystem crossings) except k_{13} and k_{30} are con-

sidered to be negligible (as in standard models for porphyrins and porphyrin-like materials),[9,20,31] the effect of neglecting an intermediate level would only be to cause the calculated relaxation rate for the modeled adjoining same-spin levels to be equal to the sum of the transition rates calculated when the intermediate level was included. When intermediate levels and all possible first-order higher intersystem crossing transitions (k_{25} and k_{51}) are both included in the model, the complexity of the model is greatly increased; however, as stated above, the presence of an intermediate level should be seen only as a strengthening of a single transition. For example, if in reality there existed an intermediate level between T_1 and T_2, and an intermediate level between S_1 and S_2, then a model that neglects intermediate levels would detect the intersystem crossing between the two aforementioned intermediate levels as an increased k_{51}, and none of the other transition rates would be affected.

Nonnegligible two-photon coefficients change the behavior of the calculated transmission curves differently from single-photon coefficients; however, two-photon coefficients do transform similarly to combinations of single-photon parameters [i.e., $\sigma_{36}^{(2)}$ yields fits to the transmission curve similarly to a combination of σ_{35}, k_{53}, and σ_{56}). Thus two-photon absorption cross sections should always provide a less flexible fit to the curve and therefore most likely will provide only an additional, extraneous, parameter to fitting the curve. In the fittings described in this paper the values of all two-photon absorption cross sections tested converged to zero. The only exception was $\sigma_{36}^{(2)}$, which converged to an exceedingly large value when k_{53} was held at a negligible value and thus was deemed to produce an unphysical solution. Further, a fitting of $\sigma_{36}^{(2)}$, when the fitting involved no constraints on k_{53}, produced no significant improvement of the calculated transmission curve. In this manner it was determined that the addition of two-photon absorption does not improve the theoretical fit. Thus for the present study the approximation of an active five-state dynamic system $(N_4 = 0, N_6 = 0, k_{25} = 0, k_{51} = 0, \sigma_{ij}^{(2)} = 0)$ was found to model successfully the transmission behavior of the [(C_6H_4–APPC)Cd]Cl solution.

Triplet–triplet annihilation is a process by which two molecules with long-lived triplet states collide in solution and annihilate each other to produce one molecule in the excited singlet and another in the ground state.[32] Two interacting solute molecules may exhibit triplet–triplet annihilation if both the solute has a long triplet lifetime and there is a relatively high solute concentration. The solute concentration used in the research reported here

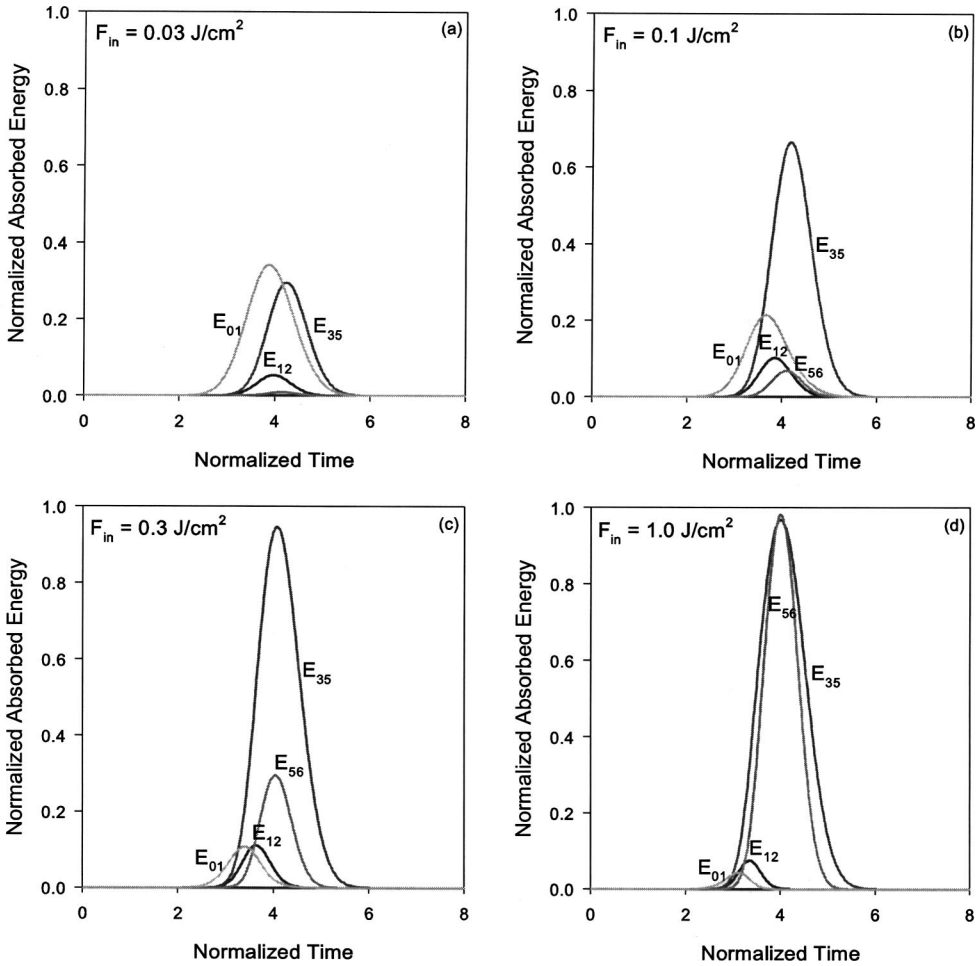

Fig. 6. Dynamics of absorbed energy at 5 ns and 532 nm for a 4.33×10^{-4} mol/L methanol solution of [(C_6H_4–APPC)Cd]Cl. Normalized absorbed energies ($E_{ij} = \sigma_{ij} N_i I$) are shown for four input fluences F_{in}.

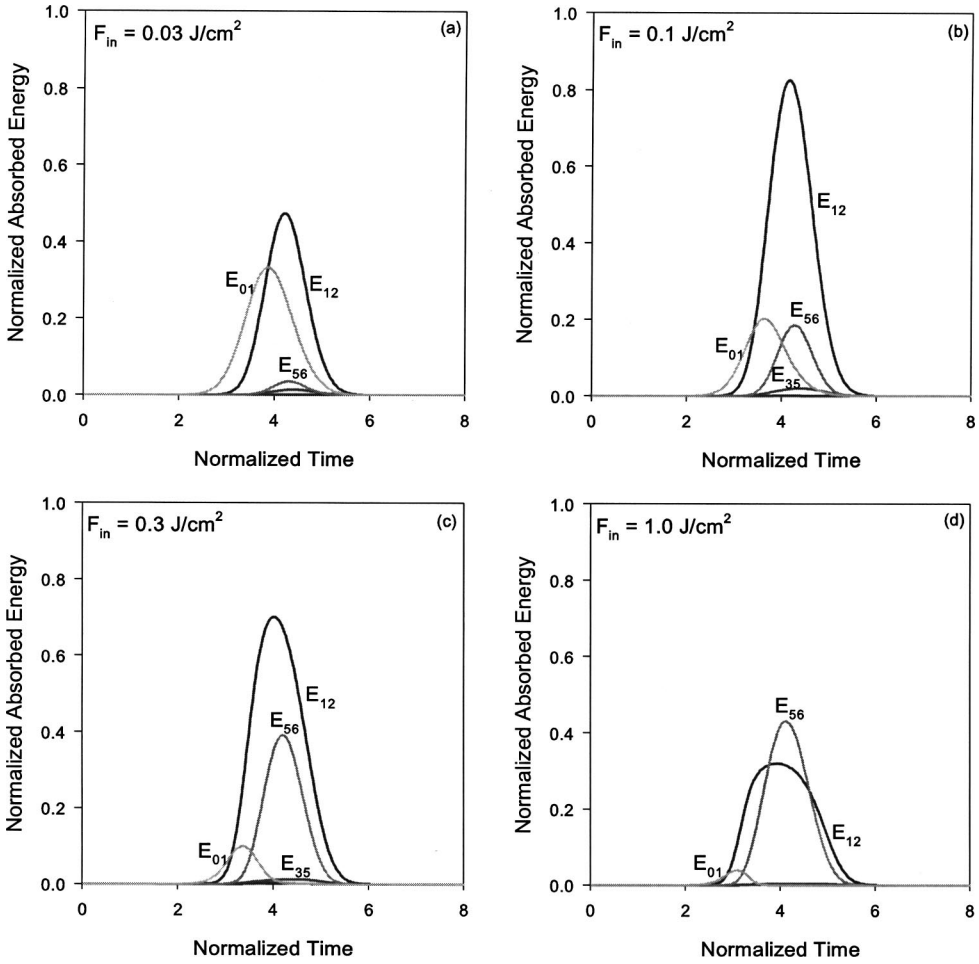

Fig. 7. Dynamics of absorbed energy at 40 ps and 532 nm for a 4.33×10^{-4} mol/L methanol solution of [$(C_6H_4$–APPC)Cd]Cl. Normalized absorbed energies ($E_{ij} = \sigma_{ij}N_iI$) are shown for four input fluences F_{in}. Because the product $\sigma_{56}N_5I$ is fairly large at high fluences, the second excited triplet state T_2 plays a much greater role in the dynamics than expected.

was relatively low. Further, the annihilation process would act only to modify k_{30} and k_{13} for T_1, or k_{25} and k_{51} for T_2; intersystem crossings involving T_2 were determined to be negligible, and T_1 mimics exactly what was measured experimentally. Thus intersolute triplet–triplet annihilation should have no effect on fitting the calculated transmission curve for the present [$(C_6H_4$–APPC)Cd]Cl complex. Triplet–triplet annihilation can occur also between a solute and a solvent molecule when the solute has an S_1 that lies below solvent S_1 and a T_1 that lies above solvent T_1. In this case the solvent–solute interaction must be strong (partially because of the presence of triplet states with highly similar energies) and the solvent molecule must attain a relatively largely populated triplet state. This situation usually occurs when the solvent and the solute are similar, which should not be the case for an APPC in methanol.

B. Absorbed Energy and Population Dynamics for [$(C_6H_4$–APPC)Cd]Cl

The relative contribution of each state can be seen through examination of the population dynamics and absorbed energy curves of the system. For 5-ns pulses, most of the population excited into S_1 quickly relaxes into T_1 through ISC; thus, triplet excited-state absorption becomes the dominant mechanism for RSA (Fig. 4). As T_1 becomes significant, RSA increases until ~0.03 J/cm^2, where N_3 surpasses N_0 and the slope of the transmission curve stabilizes. At ~1 J/cm^2, N_5 becomes significant, and thus upper triplet excited-state absorption is strongly felt. Correspondingly, a larger value of σ_{56} causes even stronger RSA in the transmission curve in the portion of the curve that is due mainly to σ_{35}. At pulse maximum for 1 J/cm^2, all or almost all of the population density is in the triplet manifold, and the ground state is bleached. For 40-ps pulses the pulse duration is much shorter than the inverse of both k_{10} and k_{13}; therefore the RSA comes predominantly from singlet excited-state absorption (Fig. 5). Similarly to the behavior for nanosecond pulses, RSA increases until ~0.03 J/cm^2, where N_1 surpasses N_0, and the slope of the transmission curve stabilizes; the steepness of this slope is dictated primarily by the dominance of larger σ_{12} over σ_{01}. At fluences of ~0.3 J/cm^2 and higher, the population of the ground state quickly becomes depleted and N_2 becomes larger than N_1 in the neighborhood of the pulse maximum; thus saturated absorption occurs because σ_{24} is less than σ_{12}. Under excitation with a 1-J/cm^2 input fluence, S_2 is the dominant state in the region of pulse excitation; however, beyond a Gaussian half-width to either side of the pulse maximum,

S_1 dominates, and the majority of the population density resides in the singlet states until a time that is approximately eight times the Gaussian half-width after the laser pulse.

The absorbed energy dynamics allow for quick determination of the relative strength of each absorption process over the pulse duration. For solutions of [(C_6H_4–APPC)Cd]Cl at 5-ns pulse excitation, the values of σ_{01} and σ_{35} are roughly equivalent; thus, for lower fluences, trends in the absorbed energy dynamics (Fig. 6) closely track those of the nanosecond population dynamics. However, at fluences above ~0.1 J/cm^2 the T_2–T_n transition begins to absorb a significant amount of energy. The T_1–T_2 transition and the T_2–T_n transition absorb almost equal amounts of energy for a pulse of F_{in} = 1 J/cm^2. The product $\sigma_{56}N_5I$ is fairly large at high fluences; thus second excited triplet state T_2 plays a much greater role in the dynamics than expected. At high fluences (and at this pulse width) it is not surprising that most of the pulse energy is absorbed into and remains in the manifold of the triplet states, because the high ISC rate and low k_{30} will effectively trap all the population density in T_1 and higher triplet states. The 40-ps dynamics for absorbed energy in methanol-solvated [(C_6H_4–APPC)Cd]Cl (Fig. 7) further emphasize the strength of influence of T_2 (a state neglected in previous models). At low fluences the dominant absorption is S_0–S_1; however, at F_{in} = ~0.02 J/cm^2 the S_1–S_2 transition becomes the dominant factor. Interestingly, although T_2 contributes to less than 10% of the total population density at approximately F_{in} = 0.5 J/cm^2, the T_2–T_n transition begins to absorb the largest portion of the energy for the pulse at this fluence. This result underscores the importance of considering all the absorption cross sections in the ESA dynamics and shows that the parameters that most strongly govern the effectiveness of methanol-solvated [(C_6H_4–APPC)Cd]Cl at more-practical device energies are the triplet state processes k_{13} and σ_{56}.

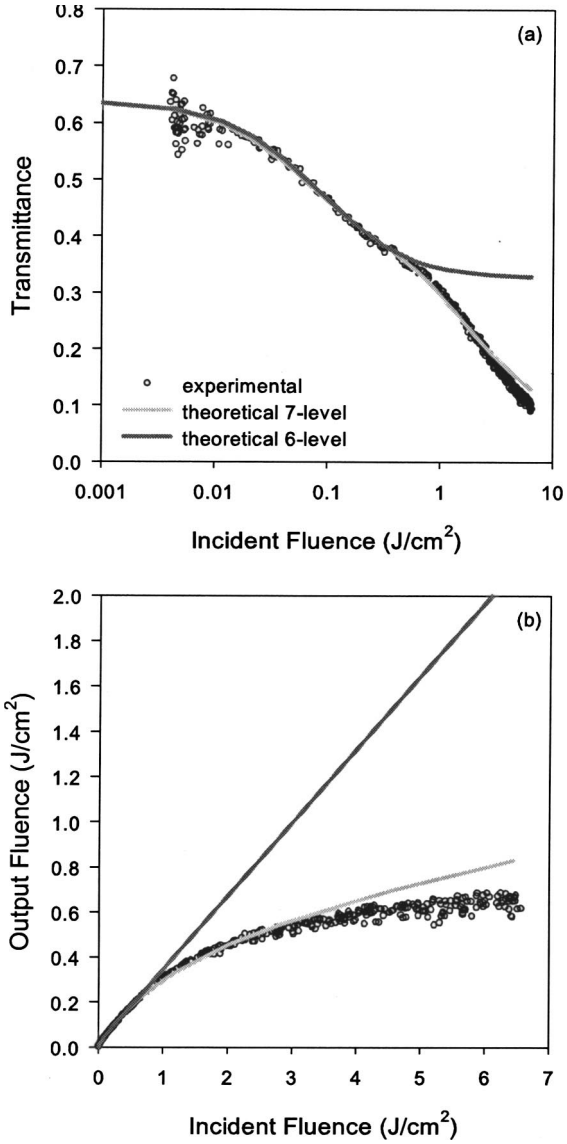

Fig. 8. As indicated, current six-state energy-level models do not adequately predict the transmission behavior of [(C_6H_4–APPC)Cd]Cl at high fluences. Without the inclusion of σ_{56} and k_{53}, the best fit to (a) the 5-ns transmission curve saturates near 0.5 J/cm^2, and values of σ_{35} are accordingly inflated. The deficiency of a six-level model is most dramatically illustrated by (b) replotting of the data as incident versus output fluence.

5. CONCLUSIONS

Previous models have successfully predicted the transmission behavior of materials that either are simpler or were measured at lower energies than the [(C_6H_4–APPC)Cd]Cl complex studied in this paper. For example, an accurate description of transmission behavior can often be achieved by fitting σ_{35} separately from σ_{12} and k_{21}; this is often done when σ_{35} is expected to be the dominant fit parameter that governs the nanosecond dynamics, and σ_{12} and k_{21} are expected to dominate the picosecond dynamics.[9,19,20] For many materials (including porphyrins) this is a fair assumption owing to the value of k_{13}. The addition of higher-order transition rates or a more-complex electronic energy-level structure may strain the reliability of a least-squares method when the separation criteria for simultaneous fitting are limited to spin character alone. A critical new step is taken in the study reported here: The core transition rates are recognized as separable not only by spin character but by fluence. At lower fluences, only the lower energy-level transitions will be active and thus only the lower energy-level parameters will govern the behavior of that portion of the transmission curve. By then expanding the fit to a larger set of parameters at higher fluences, we have already placed the full fit along a more likely well in the complex's parameter space.

The extension of measured fluence to greater than 1 J/cm^2 resulted in transmission-versus-fluence curves for the [(C_6H_4–APPC)Cd]Cl complex that cannot be fitted accurately with the six-state energy-level models currently found in the literature. Accurate fitting of the high-fluence portions of the OPL data requires a model that includes higher-order triplet transitions. At more-practical device energies, k_{13} and σ_{56} are shown to most strongly govern the excited-state population dynamics of methanol-solvated [(C_6H_4–APPC)Cd]Cl. Further, with-

out the inclusion of σ_{56} and k_{53} the best fit to the 5-ns transmission curve saturates near 0.5 J/cm^2 (Fig. 8), and values of σ_{35} are noticeably inflated. Nonlinearity that results from higher excited states can also be observed in the deviation from a cubic relationship for the phase-conjugate signal measured by degenerate four-wave mixing for this complex.[15] Accurate fitting of the dip feature in the 5-ns data for the [(C_6H_4–APPC)Cd]Cl complex indicates that the sensitivity of this curve to σ_{12} permits a more-accurate determination of the fitted parameters. Whereas similar four-, five-, and six-state energy-level models have failed to correctly model fluences larger than 1.0 J/cm^2 in texaphyrins, porphyrins, fullerenes, phthalocyanines, and naphthalocyanines,[10,31] the seven-state energy-level model presented in this paper should allow for more-accurate predictions of nonlinear absorptive behavior at high fluences for these and other similar organic reverse saturable absorbers.

ACKNOWLEDGMENTS

The authors acknowledge support under U.S. Army Research Office grant DAAD19-99-1-0119 and National Science Foundation MultiUser Instrumentation grant DBI-0070220. The authors also acknowledge the contributions that Amy Van Engen Spivey has made to the content and editing of this manuscript.

*Present address, Division of Engineering and Applied Science, California Institute of Technology, Pasadena, California 91125; e-mail, mmckerns@caltech.edu.

†Present address, Department of Chemistry, North Dakota State University, Fargo, North Dakota 58105.

REFERENCES

1. A. A. Said, C. Wamsley, D. J. Hagan, E. W. Van Stryland, B. A. Reinherdt, P. Roderer, and A. G. Dillard, "Third and fifth order optical nonlinearities in organic materials," Chem. Phys. Lett. **228**, 646–650 (1994).
2. S. M. Jensen, "The nonlinear coherent coupler," IEEE J. Quantum Electron. **QE-18**, 1580–1583 (1982).
3. D. J. Harter, M. L. Shand, and Y. B. Band, "Power/energy limiter using reverse saturable absorption," J. Appl. Phys. **56**, 865–868 (1984).
4. L. W. Tutt and T. F. Boggess, "A review of optical limiting mechanisms and devices using organics, fullerines, and semiconductors and other materials," Prog. Quantum Electron. **17**, 299–338 (1993).
5. B. G. Maiya, A. Harriman, J. L. Sessler, G. Hemmi, T. Murai, and T. E. Mallouk, "Ground- and excited-state spectral and redox properties of cadmium(II) texaphyrin," J. Phys. Chem. **93**, 8111–8115 (1989).
6. T. D. Mody and J. L. Sessler, "Texaphyrins: a new approach to drug development," J. Porphyrins Phthalocyanines **5**, 134–142 (2001).
7. R. A. Hann and D. Bloor, *Organic Materials for Nonlinear Optics* (Royal Society of Chemistry, London, 1989).
8. T. J. Bunning, L. V. Natarajan, M. G. Schmitt, B. L. Epling, and R. L. Crane, "Optical limiting in solutions of diphenyl polyenes," Appl. Opt. **30**, 4341–4350 (1991).
9. J. Si, M. Yang, Y. Wang, L. Zhang, C. Li, D. Wang, S. Dong, and W. Sun, "Nonlinear excited state absorption in cadmium texaphyrin solution," Appl. Phys. Lett. **64**, 3083–3085 (1994).
10. J. W. Perry, "Organic and metal-containing reverse saturable absorbers for optical limiters," in *Nonlinear Optics of Organic Molecules and Polymers*, H. S. Nalwa and S. Miyata, eds. (CRC Press, Boca Raton, Fla., 1997), pp. 813–840.
11. K. Mansour, P. D. Fuqua, S. R. Marder, B. S. Dunn, and J. W. Perry, "Solid state optical limiting materials based on phthalocyanine-containing polymers and organically-modified sol-gels," in *Organic, Metallo-Organic, and Polymeric Materials for Nonlinear Optical Applications*, S. R. Marder and J. W. Perry, eds., Proc. SPIE **2143**, 239–250 (1994).
12. B. G. Maiya, T. E. Mallouk, G. Hemmi, and J. L. Sessler, "Effects of substituents on the spectral and redox properties of cadmium(II) texaphyrins," Inorg. Chem. **29**, 3738–3745 (1990).
13. W. Sun, C. C. Byeon, M. M. McKerns, C. M. Lawson, G. M. Gray, and D. Wang, "Optical limiting performances of asymmetric pentaazadentate porphyrin-like cadmium complexes," Appl. Phys. Lett. **73**, 1167–1169 (1998).
14. W. Sun, C. C. Byeon, M. M. McKerns, C. M. Lawson, G. M. Gray, and D. Wang, "Relationship between chemical structures and optical limiting properties of penta-azadentate porphyrinlike metal complexes," in *Nonlinear Optical Liquids for Power Limiting and Imaging*, C. M. Lawson, ed., Proc. SPIE **3472**, 127–134 (1998).
15. W. Sun, C. C. Byeon, C. M. Lawson, G. M. Gray, and D. Wang, "Third-order susceptibilities of asymmetric pentaazadentate porphyrin-like metal complexes," Appl. Phys. Lett. **74**, 3254–3256 (1999).
16. W. Sun, C. C. Byeon, M. M. McKerns, C. M. Lawson, S. Dong, D. Wang, and G. M. Gray, "Characterization of the third-order nonlinearity of [(CH_3–TXP)Cd]Cl," in *Power-Limiting Materials and Devices*, C. M. Lawson, ed., Proc. SPIE **3798**, 107–116 (1999).
17. J. Si, "Excited state optical nonlinearity in metallo-porphyrin-like and its applications," Ph.D. dissertation (Harbin Institute of Technology, Harbin, China, 1994).
18. W. Sun, C. C. Byeon, C. M. Lawson, G. M. Gray, and D. Wang, "Third-order nonlinear optical properties of an expanded porphyrin cadmium complex," Appl. Phys. Lett. **77**, 1759–1761 (2000).
19. C. R. Giuliano and L. D. Hess, "Nonlinear absorption of light: optical saturation of electronic transitions in organic molecules with high intensity laser radiation," IEEE J. Quantum Electron. **QE-3**, 358–367 (1967).
20. J. Si, M. Yang, Y. Wang, L. Zhang, C. Li, D. Wang, S. Dong, and W. Sun, "Nonlinear absorption in metallo-porphyrin-like," Opt. Commun. **109**, 487–491 (1994).
21. A. Jasat and D. Dolphin, "Expanded porphyrins and their heterologs," Chem. Rev. **97**, 2267–2340 (1997).
22. J. L. Sessler, M. R. Johnson, and V. J. Lynch, "Synthesis and crystal structure of a novel tripyrrane-containing porphyrinogen-like macrocycle," J. Org. Chem. **52**, 4394–4397 (1987).
23. W. Sun and D. Wang, "The synthesis and characterization of asymmetric pentaazadentate porphyrin-like metal complexes," Chin. Chem. Lett. **4**, 225–228 (1993).
24. W. Sun and D. Wang, "The synthesis and characterization of asymmetric pentaazadentate porphyrin-like metal complexes," Chin. J. Org. Chem. **14**, 34–38 (1994).
25. Q. Gong, Y. Wang, S.-C. Yang, Z. Xia, Y. H. Zou, W. Sun, S. Dong, and D. Wang, "Third-order optical nonlinearities of new two-dimensional pi-conjugated metal-coordinated complexes," J. Phys. D **27**, 911–913 (1994).
26. W. Sun and D. Wang, "Excited-state properties of asymmetric pentaazadentate expanded porphyrins," Science in China B **39**, 509–518 (1996).
27. C. C. Byeon, M. M. McKerns, W. Sun, T. M. Nordlund, C. M. Lawson, and G. M. Gray, "Excited state lifetime and intersystem crossing rate of asymmetric pentaazadentate porphyrin-like metal complexes," Appl. Phys. Lett. **84**, 5174–5176 (2004).
28. M. M. McKerns, "Characterization of molecular structure, excited-state absorption, and nonlinear optical response of metallotexaphyrin complexes," Ph.D. dissertation (University of Alabama at Birmingham, Birmingham, Ala., 2002).
29. K. Mansour, D. Alvarez, Jr., K. J. Perry, I. Choong, S. R.

Marder, and J. W. Perry, "Dynamics of optical limiting in heavy-atom-substituted phthalocyanines," in *Organic and Biological Optoelectronics*, P. M. Rentzepis, ed., Proc. SPIE **1853**, 132–141 (1993).
30. T. H. Wie, D. J. Hagan, M. J. Sence, E. W. Van Stryland, J. W. Perry, and D. R. Coulter, "Direct measurements of nonlinear absorption and refraction in solution of phthalocyanines," Appl. Phys. B **54**, 46–51 (1992).
31. R. L. Sutherland, *Handbook of Nonlinear Optics* (Marcel Dekker, New York, 1996).
32. N. J. Turro, *Modern Molecular Photochemistry* (University Science, Sausalito, Calif., 1991).